SCIENTIFIC REPORTS

OPEN

SUBJECT AREAS:
COMPOSITES
ELECTRONIC DEVICES

Received
5 August 2013

Accepted
15 May 2014

Published
12 June 2014

Correspondence and requests for materials should be addressed to L.S.C. (lishancui63@126.com) or Y.R. (ren@aps.anl.gov)

A novel multifunctional NiTi/Ag hierarchical composite

Shijie Hao[1], Lishan Cui[1], Jiang Jiang[1], Fangmin Guo[1], Xianghui Xiao[2], Daqiang Jiang[1], Cun Yu[1], Zonghai Chen[3], Hua Zhou[2], Yandong Wang[4], YuZi Liu[5], Dennis E. Brown[6] & Yang Ren[2]

[1]State Key Laboratory of Heavy Oil Processing and Department of Materials Science and engineering, China University of Petroleum, Beijing 102249, China, [2]X-ray Science Division, Advanced Photon Source, Argonne National Laboratory, Argonne, Illinois 60439, USA, [3]Chemical Sciences and Engineering Division, Argonne National Laboratory, Argonne, Illinois 60439, USA, [4]State Key Laboratory for Advanced Metals and Materials, University of Science and Technology, Beijing 100083, China, [5]Center for Nanoscale Materials, Argonne National Laboratory, Argonne, Illinois 60439, USA, [6]Department of Physics, Northern Illinois University, De Kalb, Illinois 60115, USA.

Creating multifunctional materials is an eternal goal of mankind. As the properties of monolithic materials are necessary limited, one route to extending them is to create a composite by combining contrasting materials. The potential of this approach is neatly illustrated by the formation of nature materials where contrasting components are combined in sophisticated hierarchical designs. In this study, inspired by the hierarchical structure of the tendon, we fabricated a novel composite by subtly combining two contrasting components: NiTi shape-memory alloy and Ag. The composite exhibits simultaneously exceptional mechanical properties of high strength, good superelasticity and high mechanical damping, and remarkable functional properties of high electric conductivity, high visibility under fluoroscopy and excellent thermal-driven ability. All of these result from the effective-synergy between the NiTi and Ag components, and place the composite in a unique position in the properties chart of all known structural-functional materials providing new opportunities for innovative electrical, mechanical and biomedical applications. Furthermore, this work may open new avenues for designing and fabricating advanced multifunctional materials by subtly combining contrasting multi-components.

Advances in technology need urgently the development of high-performance materials having exceptional mechanical properties and remarkable functional properties, which are very important for realizing the miniaturization and simplification of devices. Unfortunately, the properties such as strength, toughness, damping, conductivity, etc. tend to be reciprocally exclusive, and accomplishing optimal performance is invariably a compromise confined by the existing empirical designs. It is noted that the nature materials like tendon, bone, nacre and wood created by billions of years of evolution usually achieve perfect structural and functional integrity through subtly combining the contrasting materials that possess distinctly different properties[1,2]. The approach to creating multifunctional materials by combining contrasting components is lively illustrated by the formation of bio-minerals where organic macromolecules are combined with brittle minerals to create materials having high strength, toughness and damping[1,2]. Nature has been a school for scientists and engineers, and learning from nature has long been a source of bio-inspiration for human beings[3–12].

NiTi shape-memory alloys (SMAs), due to their excellent shape-memory effect, superelasticity and biocompatibility, are used for many products, such as cellular phone antennae, spectacle frames, medical guidewires and stents[13–15]. Unfortunately, conventional NiTi SMAs exhibit also high electrical resistance, low mechanical damping and low visibility under fluoroscopy[16,17], which severely limit their usefulness in applications. Ag has good visibility under fluoroscopy and is one of the best electrically conductive materials possessing high electrical conductivity. Thus, it is predicted that the composites made with the NiTi and Ag components may simultaneously have excellent shape-memory effect, superelasticity, high conductivity and good visibility under fluoroscopy. Many attempts have been made to achieve such composites with exceptional properties, but all results obtained so far are far from desirable[18–20]. One reason is that, in the composites fabricated by melting, adding elemental Ag significantly changes the phase transformation behavior of NiTi matrix, and thereby affects the shape-memory effect and superelasticity. Another reason is that the Ag component in the composites is discontinuous, and thereby contributes little to the electrical conductivity of composites.

In this study, inspired by the hierarchical design of the tendon, we achieved a novel NiTi/Ag composite wire by repeated assembling and wire-drawing. The Ag fibers are continuous and are regularly dispersed and well aligned

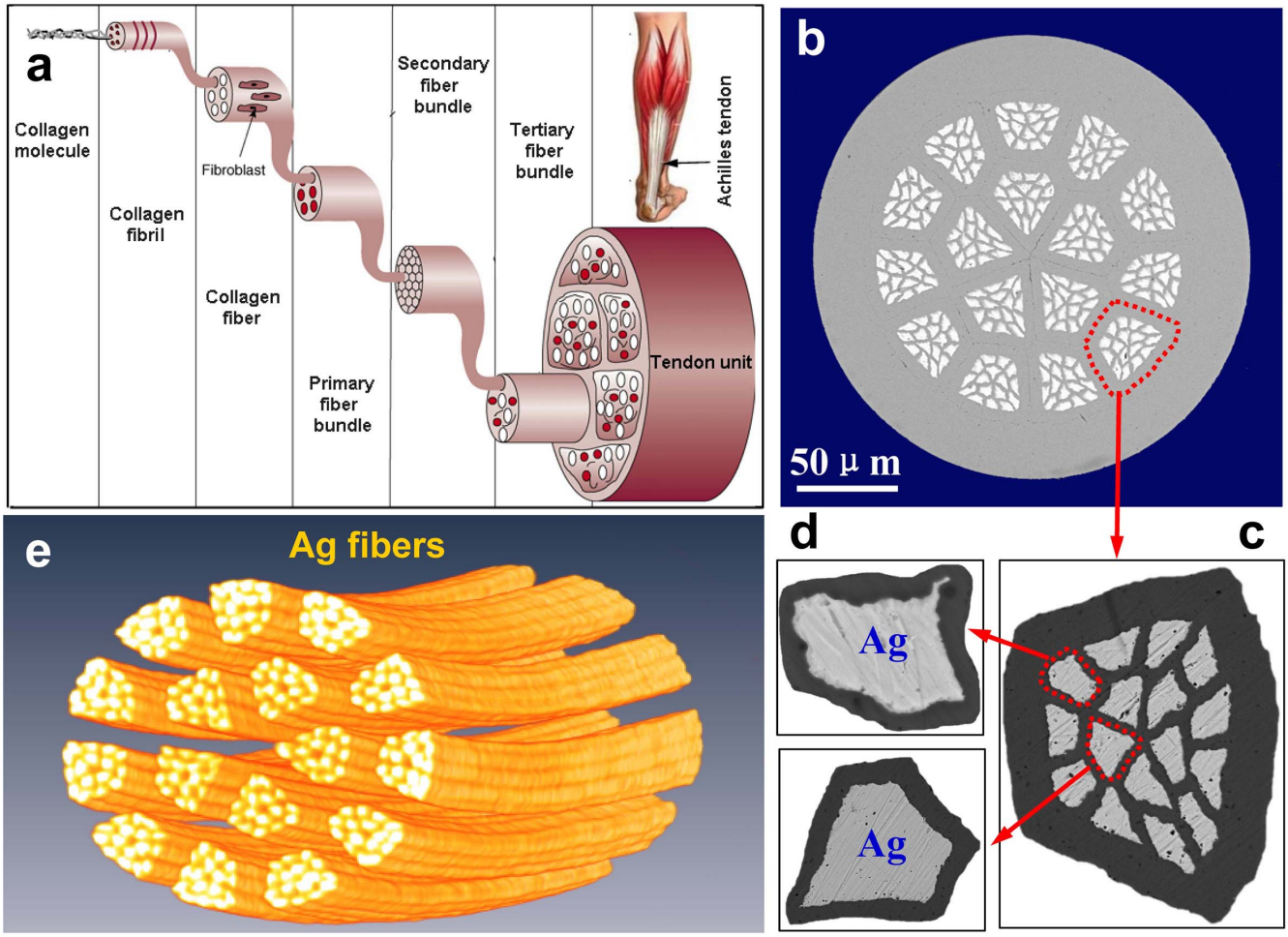

Figure 1 | Typical microstructure of tendon and the NiTi/Ag composite. (a), Schematic illustration of the hierarchical structure of tendon (Fig. 1a is from Silver et. al's paper *J Biomech.* 39, 1563–1582 (2006))[21]. (b), Scanning electron morphology (SEM) image of the cross-section of the composite wire (bright regions: cross sections of Ag fibers; dark regions: NiTi matrix). (c–d), Successive views of the hierarchical structure of the composite. (e), Three-dimensional (3-D) high-energy X-ray tomography image of the Ag fibers embedded in the composite.

in the NiTi SMA matrix along the wire axial direction. The composite simultaneously exhibits exceptional mechanical properties of high-strength, good superelasticity and high mechanical damping, and remarkable functional properties of high-conductivity, high visibility under fluoroscopy and excellent thermal-driven ability. These exceptional properties are believed to result from the effective-synergy of the NiTi and Ag contrasting components, and render the composite great potential for innovative electrical, mechanical and biomedical applications.

Results and Discussion

Fabrication. The NiTi/Ag hierarchical composite wire was fabricated by repeated assembling and wire-drawing. A pure Ag wire of 1.6 mm in diameter was inserted into a superelastic NiTi tube with an inner diameter of 1.7 mm and an outer diameter of 2.2 mm, and then they were cold-drawn into a thin wire of 0.36 mm in diameter at room temperature with multiple times of intermediate electric annealing at 750°C for 20 seconds. The cold-drawn thin wire was cut into 16 wires with 500 mm in length, and then they were inserted into the NiTi tube with the same size as the initial one. The same assembling and wire-drawing processes were repeated several times (1–5 times) to obtain the NiTi/Ag hierarchical composite wires (Fig. S1) with different levels of hierarchy (Figs. S2 and S3). The test samples were cut from the cold-drawn wire and subsequently annealed at 330°C for 20 min followed by air cooling.

Microstructure. The NiTi/Ag composite is highly comparable to the tendon in morphology (Fig. 1a)[21]. The scanning electron morphology (SEM) image of the cross-section of the composite wire with two levels of hierarchy is shown in Fig. 1b and the successive views of the hierarchical structure are shown in Figs. 1c–d. To better understand this hierarchical structure, synchrotron high-energy X-ray tomography was used to visualize the three-dimensional (3-D) images of the Ag fibers embedded in the composite, as shown in Fig. 1e and Fig. S4. It can be seen that the Ag fibers of ~4.0 μm in diameter are continuous and are regularly dispersed and well aligned in the NiTi matrix along the longitude axial direction. From the SEM images, it can be calculated that the volume fractions of the Ag and NiTi components are about 12% and 88%, respectively. The component composition and distribution of the composite measured by energy dispersive X-ray spectroscopy (EDX) are shown in Fig. S5, indicating that there is no visible mixture existing between the NiTi and Ag components. The high-energy X-ray diffraction measurements of the composite are shown in Fig. S6, indicating that the composite consists of B2-NiTi and face-centered cubic Ag phases.

Mechanical properties. The typical mechanical behavior of the NiTi/Ag composite with two levels of hierarchy, after a pre-treatment of a tensile strain cycle of 8%, is shown in Fig. 2a. For comparison, the tensile stress-strain curve of a pure Ag wire is also presented in Fig. 2a. It is observed that the NiTi/Ag composite exhibits a recoverable strain of over 7%, yield strength of

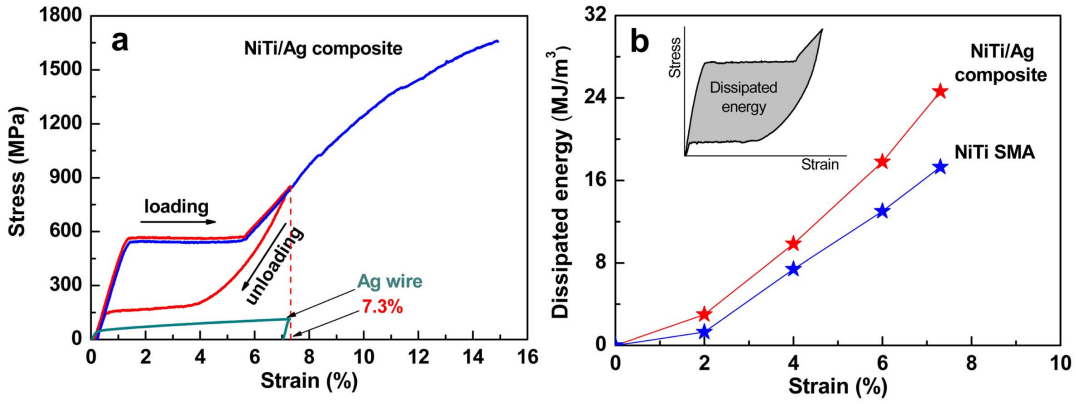

Figure 2 | Typical mechanical properties of the NiTi/Ag composite. (a), Uniaxial tensile stress-strain curve of the composite (blue curve), and cyclic tensile stress-strain curves of the composite (red curve) and a pure Ag wire (green curve) obtained at room temperature. (b), The dissipated energy per unit volume by one superelastic cycle as a function of applied strain for the composite and a commercial NiTi SMA wire.

~560 MPa and break strength of ~1650 MPa. The recoverable strain range is much larger than that of the Ag wire (~0.3%). The yield strength is also higher than that of the Ag wire (~50 MPa). Compared to the well-known high damping NiTi SMAs[22], the composite exhibits a higher mechanical damping capability during tensile cycling. The absorbed energy by a superelastic cycle as a function of applied strain for the composite and a commercial NiTi wire are shown in Fig. 2b. The dissipated energy in one deformation cycle can be denoted by the area of the hysteresis loop (the inset of Fig. 2b). One can see that the dissipated energy for the composite subjected to 7% strain is up to 23.8 MJ/m^3, which is larger than that of the commercial NiTi wire (~14.6 MJ/m^3).

To reveal the mechanism of the exceptional mechanical behavior, *in-situ* high-energy X-ray diffraction (HE-XRD)[23,24] was carried out on the composite throughout the pre-treatment and subsequent tensile cycle (Fig. 3a). Fig. 3b shows the *in-situ* HE-XRD patterns of the composite obtained during tensile cycling. Figs. 3c, 3d and 3e exhibit the *d*-spacing strains for the Ag (111), B2-NiTi (110) and B19′-NiTi (001) planes perpendicular to the loading direction versus the applied strain, respectively. Based on the HE-XRD results, it is found that the superelasticity of the NiTi/Ag composite results from the effective combination of the reversible stress-induced martensitic transformation (SIMT) deformations of NiTi matrix and the tensile and compressive elastic-plastic deformations of Ag fibers during tensile cycling, which is similar to that of the NiTi-sheath/Cu-core composite reported[25].

Upon the tensile loading of the pre-treatment, the NiTi matrix sequentially underwent the tensile elastic deformation of austenite, the SIMT deformation (B2 → B19′)[13,14] and the tensile elastic deformation of oriented martensite. The Ag fibers underwent a small tensile elastic deformation (O-A in Fig. 3c) followed by a large tensile plastic deformation (A–B in Fig. 3c). Upon the unloading, the NiTi matrix sequentially underwent the tensile elastic strain recovery of oriented martensite, the reverse SIMT deformation (B19′ → B2)[13,14] and the tensile elastic strain recovery of austenite. The Ag fibers underwent a small tensile elastic strain recovery (B–C in Fig. 3c) followed by a small compressive elastic deformation (C–D in Fig. 3c) and a large compressive plastic deformation (D–E in Fig. 3c). Upon the tensile loading of the subsequent cycle, the NiTi matrix underwent a smaller elastic deformation ('C–D' in Fig. 3d) compared to that in the pre-treatment ('A–B' in Fig. 3d), while the Ag fibers experienced a mixed elastic deformation ('E–G' in Fig. 3c) consisting of a compressive elastic deformation of ~0.13% ('E–F' in Fig. 3c) and a tensile elastic deformation of ~0.19% ('F–G' in Fig. 3c). Except for the elastic deformation, both the NiTi and Ag components in the subsequent cycle show the similar deformation behavior to that in the pre-treatment.

From the above results and analysis, it is found that the Ag fibers underwent the tensile/compressive plastic deformations during tensile cycling, thus it is expected that the tensile/compressive plastic deformations of the Ag fibers during tensile cycling would cause large mechanical energy dissipation. Therefore, the high mechanical damping of the NiTi/Ag composite may mainly originate from the energy dissipation in the reversible SIMT of NiTi matrix and the plastic deformation of Ag fibers during tensile cycling.

Electrical properties. The NiTi/Ag composite possesses a high electrical conductivity which is at least 4 orders higher than that of the existing stretchable conductive materials made with elastomeric matrices. Stretchable conductors have attracted broad attention recently because they play a key role in the development of stretchable electronics such as flexible displays, stretchable circuits, functional electronic eyes, and so on[25–29]. Two strategies have been used to fabricate stretchable conductors: one is to fabricate wavy or net-shaped conductive structures by releasing pre-strained rubber substrate with conductive materials lying on it, and the other is to disperse conductive material in rubber matrix. However, compared to common metal conductors such as Cu, Ag and Al, the existing stretchable conductors prepared by the above two methods exhibit poor electrical conductivity (0.01 ~ 10 S/cm) and low strength (1 ~ 10^2 MPa)[29,30], which severely limit their applications in the areas requiring high-strength, high-elasticity and high-conductivity. Here, the NiTi/Ag hierarchical composite not only has a high yield strength (~560 MPa) and a large recoverable strain (>7%) but also possesses a high electrical conductivity of ~1.2*10^5 S/cm that is almost comparable in magnitude to that of pure Ag (~6.3*10^5 S/cm) and is at least 4 orders higher than that of the existing stretchable conductors made with elastomeric matrices. Based on the observations on the morphology of the NiTi/Ag composite (Fig. 1), we knew that the Ag fibers were continuous in the composite, thus the composite's high electrical conductivity can be attributed to the large contribution of the continuous Ag fibers. Fig. 4a shows the electrical resistance of the composite (normalized to its initial resistance at zero strain) versus the applied macroscopic strain. It is observed that the electrical resistance of the composite is reversible upon the loading and unloading. According to the reversibility of resistance, the main reasons for the change of resistance with applied strain should be derived from the changes in the cross-sectional area, length and internal stress of the composite wire during tensile cycling[25]. The unique combinations of the high-strength, good superelasticity and high-conductivity place the NiTi/Ag composite in a unique position in the properties chart of electrically conductive materials (Fig. 4b).

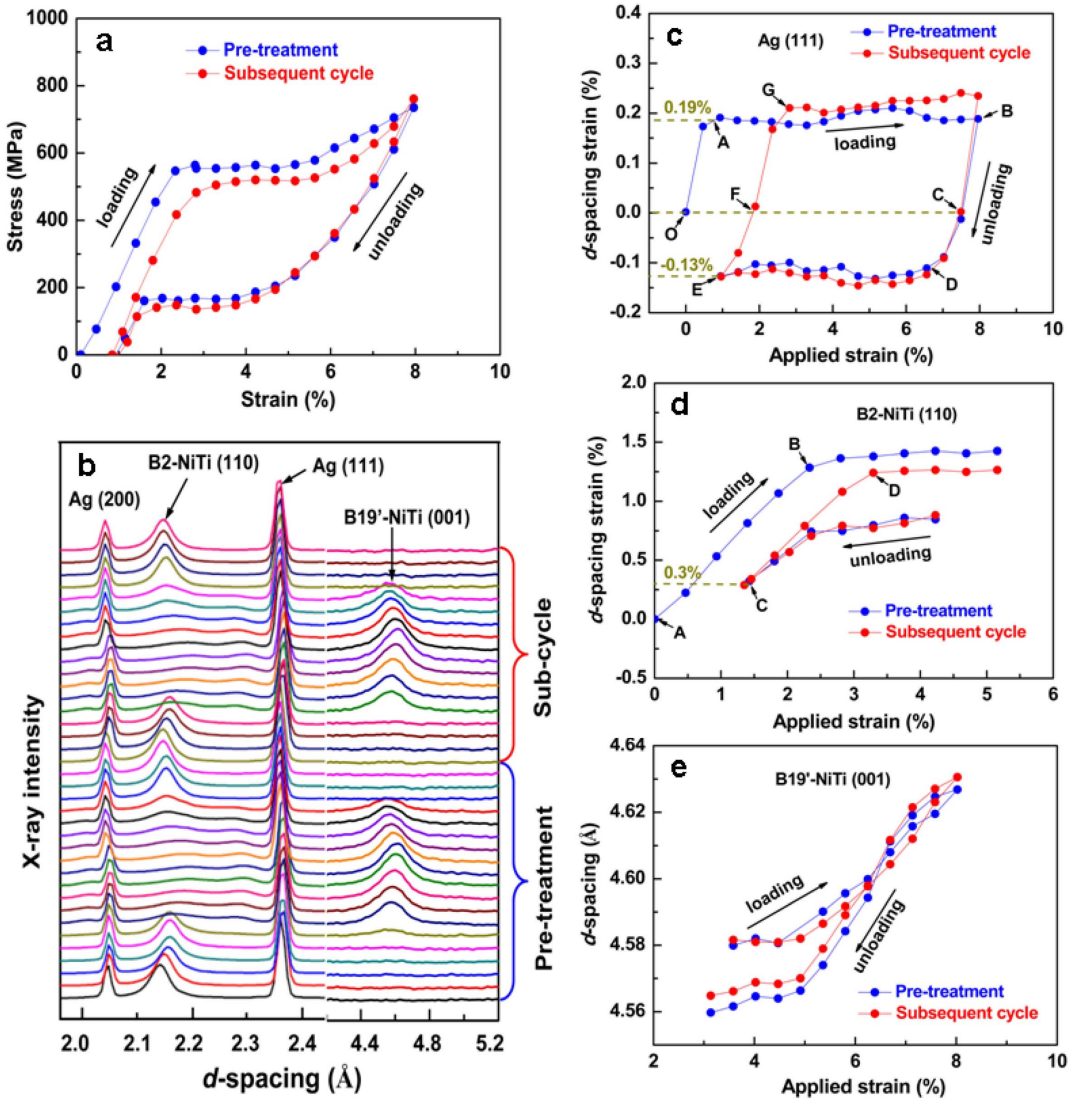

Figure 3 | ***In-situ*** **synchrotron X-ray diffraction results of the NiTi/Ag composite in the pre-treatment and subsequent tensile cycle.** (a), Tensile cyclic stress-strain curves. (b), Evolution of diffraction patterns throughout the pre-treatment and subsequent cycle. (c–d), Evolutions of the *d*-spacing strains for Ag (111) and B2-NiTi (110) planes perpendicular to the loading direction with applied strain. (e), Plot of the *d*-spacing of B19′-NiTi (001) plane perpendicular to the loading direction versus applied strain. Note: it is difficult to define the *d*-spacing of B19′-NiTi (001) plane without stress, thus we plot the *d*-spacing of B19′-NiTi (001) plane versus applied stain rather than the *d*-spacing strain of B19′-NiTi (001).

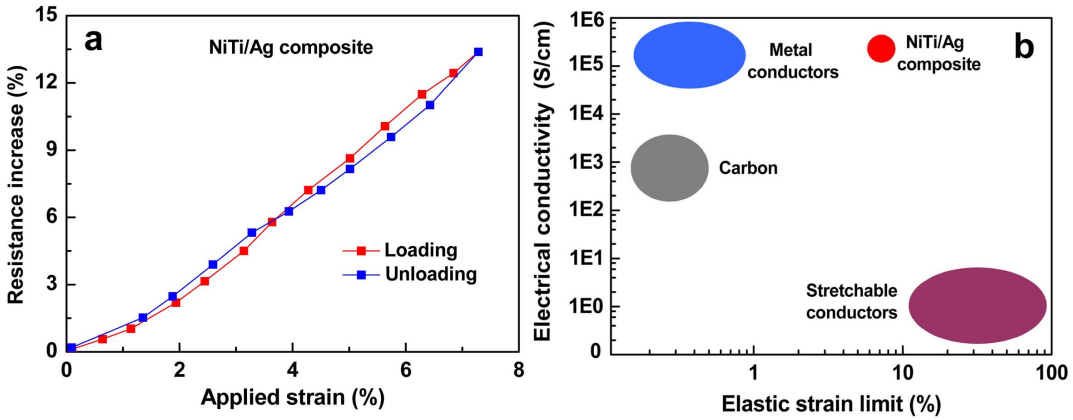

Figure 4 | **Typical electrical properties of the NiTi/Ag composite.** (a), Electrical resistance change of the composite as a function of the applied strain in the tensile cycle. (b), Comparison of electrical conductivity as a function of the elastic strain limit for metal conductors, carbon, existing stretchable conductors and the NiTi/Ag composite.

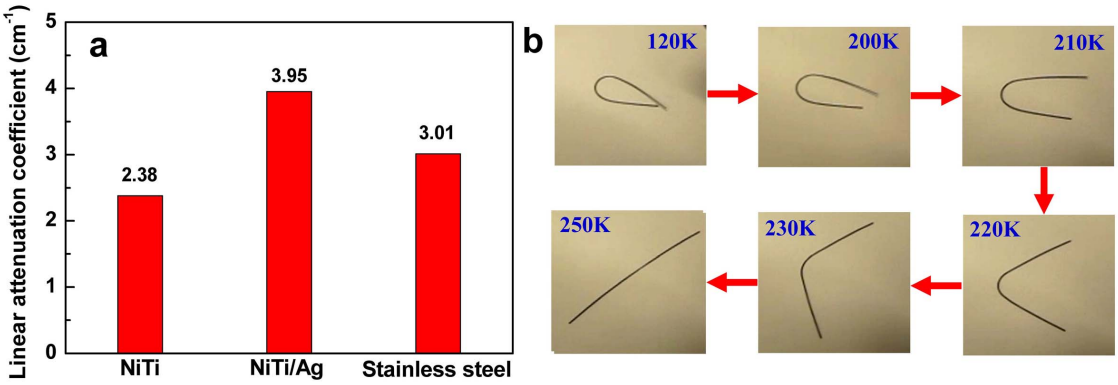

Figure 5 | Visibility under fluoroscopy and thermal-driven ability of the NiTi/Ag composite. (a), Comparison of the linear attenuation coefficients for 100 keV X-rays of the NiTi/Ag composite, pure NiTi and 316L stainless steel. (b), Thermal-driven process of the NiTi/Ag composite on heating.

Visibility under fluoroscopy. It is known that NiTi SMA is one of the most important implant materials in biomedical applications. To analyze the motion of implants, it is crucial to accurately monitor their 3-D positions and orientations using radiography. However, small NiTi stents, guidewires and catheters sometimes do not provide satisfactory visibility under fluoroscopy[17,31]. The methods to enhance the visibility include adding a mark of noble metals and coating with gold[17,32,33]. Although these methods improved the radiopacity, problems such as risks of galvanic corrosion and hydrogen embrittlement still exist[34]. In this study, we calculated the high-energy X-ray absorption coefficients at 100 Kev for pure NiTi, NiTi/Ag composite and 316L stainless steel, based on their composition, density and the mass attenuation coefficient data obtained from the NIST Standard Reference Database. Fig. 5a shows the linear attenuation coefficient, μ, for the three systems (μ = 2.38, 3.95 and 3.01 cm^{-1} for NiTi, NiTi/Ag and 316L stainless steel, respectively). One can see that the NiTi/Ag composite possesses a much better radiopacity than pure NiTi and even the 316L stainless steel that extensively used as an implant material having high visibility under fluoroscopy. Moreover, the Ag fibers are well wrapped in the NiTi matrix, which well avoids the risks of galvanic corrosion and hydrogen embrittlement. Besides the good visibility under fluoroscopy, the composite retains good superelasticity (Fig. 3a) and thermal-driven ability (Fig. 5b). Thus, the excellent integrated performance renders the composite great potential for future biomedical applications.

Conclusions

Inspired by nature's hierarchical structure of the tendon, we achieved a novel NiTi/Ag composite fabricated by assembling, wire drawing and mechanical pre-treatment. The composite simultaneously exhibits exceptional mechanical properties of high strength, good superelasticity and high mechanical damping, and remarkable functional properties of high conductivity, high visibility under fluoroscopy and excellent thermal-driven ability. These exceptional properties are attributed to the effective-synergy between the NiTi and Ag components, and open new opportunities for innovative electrical, mechanical and biomedical applications. For instance, the composite can be used as artificial tendons for robotic eyes and hands, or structural supports acting as shock absorbers for robotic legs, requiring a high elasticity, a high modulus, and a high mechanical damping as well as an electrical pathway for sensory measurements and feedback. The composite also can be used for small biomedical devices requiring high-visibility under fluoroscopy, high-strength, high-elasticity and excellent thermal-driven ability. Moreover, due to the unique combination of high strength, good superelasticity and high conductivity, the composite has great potential to be used as high-strength stretchable electric wires and cables.

More broadly, we provide a feasible route to prepare a wide variety of multifunctional materials by subtly combining various contrasting components, as shown in Fig. S7. The method developed in this study has two key advantages compared to other methods[18–20]: one is all components being continuous in the composites; another is no mixing between different components, thereby each component can retain its own characteristics in the composites. Thus, it can be predicted that if we select a NiTi SMA to combine with a functional component with exceptional magnetic (or superconductive) property to fabricate a new composite, this material should simultaneously possesses excellent thermal-driven ability, superelasticity and superior magnetic (or superconductive) properties.

Methods

In-situ synchrotron X-ray diffraction was performed at the 11-ID-C beamline of the Advanced Photon Source (APS) at Argonne National Laboratory. High-energy X-rays of 115 keV energy and 0.4 mm × 0.4 mm beam size were used to obtain two-dimensional diffraction patterns in the transmission geometry using a Perkin-Elmer large area detector placed at 1.8 m from the sample. In-situ tensile deformation was performed using an Instron testing machine at a strain rate of 1×10^{-4} s^{-1} and the total elongation of the gauge length was measured with a static axial clip-on extensometer. Gaussian fits were used to determine diffraction peak positions. The error of the d-spacing strain is smaller than 0.05%. X-ray tomography measurements were conducted at 2-BM beamline of APS. Pink beam was applied with peak energy at about 60 keV. PCO.dimax CMOS camera with Mitutoyo 10× lens was employed for recording projection images, which gives 1.1 μm effective pixel size. SEM images were taken using a FEI Quanta 200F scanning electron microscope operated at a voltage of 20 kV. The 4-probe resistance measurements were used to measure the resistance of the NiTi/Ag hierarchical composite wire. The composite wire was repeatedly stretched and released by a tensile testing stage and the gauge length was measured with a static axial clip-on extensometer, while the electric resistance was measured at the same time by a digital multimeter (Keithley, 34401A). The test error of electrical resistance is about 2%.

1. Fratzl, P. & Weinkamer, R. Nature's hierarchical materials. *Prog. Mater. Sci.* **52**, 1263–1334 (2007).
2. Meyers, M., Chen, P.-Y., Lin, A. & Seki, Y. Biological materials: Structure and mechanical properties. *Prog. Mater. Sci.* **53**, 1–206 (2008).
3. Lee1, S. *et al.* A monolithically integrated plasmonic infrared quantum dot camera. *Nat. Commum.* **2**, 286 (2011).
4. Finnemore, A. *et al.* Biomimetic layer-by-layer assembly of artificial nacre. *Nat. Commum.* **3**, 966 (2012).
5. Sun, J. *et al.* Bioinspired hollow semiconductor nanospheres as photosynthetic nanoparticles. *Nat. Commum.* **3**, 1139 (2012).
6. Jen, Y.-J. *et al.* Biologically inspired achromatic waveplates for visible light. *Nat. Commum.* **2**, 363 (2011).
7. Tang, Z., Kotov, A. N., Magonov, S. & Ozturk, B. Nanostructured artificial nacre. *Nat. Mater.* **2**, 413–418 (2003).
8. Pouget, E. *et al.* Hierarchical architectures by synergy between dynamical template self-assembly and biomineralization. *Nat. Mater.* **6**, 434–439 (2007).
9. Capadona, J. R., Shanmuganathan, K., Tyler, D. J., Rowan, S. J. & Weder, C. Stimuli-Responsive Polymer Nanocomposites Inspired by the Sea Cucumber Dermis. *Science* **319**, 1370–1374 (2008).
10. Chung, W.-J. *et al.* Biomimetic self-templating supramolecular structures. *Nature* **478**, 364–368 (2011).

11. Munch, E. *et al.* Tough, Bio-Inspired Hybrid Materials. *Science* **322**, 1516–1520 (2008).
12. Yoo, J.-W., Irvine, D. J., Discher, D. E. & Mitragotri, S. Bio-inspired, bioengineered and biomimetic drug delivery carriers. *Nat. Rev.* **10**, 521–535 (2011).
13. Otsuka, K. & Ren, X. Physical metallurgy of Ti–Ni-based shape memory alloys. *Prog. Mater. Sci.* **50**, 511–678 (2005).
14. Otsuka, K. & Wayman, C. M. *Shape Memory Materials* (Cambridge University Press, Cambridge, 1998).
15. Duerig, T., Pelton, A. & Stöckel, D. An overvIew of nitinol medical applications. *Mater. Sci. Eng., A* **273–275**, 149–160 (1999).
16. Lin, Z., Hsiao, H., Mackiewicz, D., Anukhin, B. & Kelly Pike. Anisotropic Behavior of Radiopaque NiTiPt Hypotube for Biomedical Applications. *Adv. Eng. Mater.* **11**, B189–193 (2009).
17. Cheng, Y., Cai, W., Li, H. L. & Zheng, Y. F. Surface modification of NiTi alloy with tantalum to improve its biocompatibility and radiopacity. *J Mater Sci.* **41**, 4961–4964 (2006).
18. Bitzer, M., Bram, M., Buchkremer, H. P. & Stover, D. Phase Transformation Behavior of Hot Isostatically Pressed NiTi-X (X = Ag, Nb, W) Alloys for Functional Engineering Applications. *J Mater Eng Perform.* **21**, 2535–2545 (2012).
19. Oh, K. T., Joo, U. H., Park, G. H., Hwang, C. J. & Kim, K. N. Effect of silver addition on the properties of nickel-titanium alloys for dental application. *J. Biomed. Mater. Res. B.* **76**, 306–314 (2006).
20. Zheng, Y. F. *et al.* Introduction of antibacterial function into biomedical TiNi shape memory alloy by the addition of element Ag. *Acta Biomater.* **7**, 2758–2767 (2011).
21. Wang, H.-C. J. Mechanobiology of tendon. *J Biomech.* **39**, 1563–1582 (2006).
22. Midller, I. & Xu, H. On the pseudo-elastic hysteresis. *Acta Metall Mater.* **39**, 263–271 (1991).
23. Hao, S. J. *et al.* The ultrahigh mechanical energy-absorption capability evidenced in a high-strength NbTi/NiTi nanocomposite. *Appl. Phys. Lett.* **99**, 024102 (2011).
24. Hao, S. J. *et al.* Phase-stress partition and stress-induced martensitic transformation in NbTi/NiTi nanocomposite. *Appl. Phys. Lett.* **99**, 084103 (2011).
25. Hao, S. J. *et al.* A Novel Stretchable Coaxial NiTi-Sheath/Cu-Core Composite with High Strength and High Conductivity. *Adv. Mater.* **25**, 1199–1202 (2013).
26. Rogers, A. J., Someya, T. & Huang, G. Y. Materials and mechanics for stretchable electronics. *Science* **327**, 1603–1607 (2010).
27. Sekitani, T. *et al.* Stretchable active-matrix organic light-emitting diode display usingprintable elastic conductors. *Nat.Mater.* **8**, 494–499 (2009).
28. Yu, C., Masarapu, C., Rong, J., Wei, B. & Jiang, H. Stretchable supercapacitors based on buckled single-walled carbon nanotube macrofilms. *Adv. Mater.* **21**, 4793–4797 (2009).
29. Sekitani, T. *et al.* A rubberlike stretchable active matrix using elastic conductors. *Science* **321**, 1468–1472 (2008).
30. Shin, M. K. *et al.* Elastomeric conductive composites based on carbon nanotube forests. *Adv. Mater.* **22**, 2663–2667 (2010).
31. Lin, Z., Hsiao, H., Mackiewicz, D., Anukhin, B. & Kelly Pike. Anisotropic Behavior of Radiopaque NiTiPt Hypotube for Biomedical Applications. *Adv. Eng. Mater.* **11**, B189–193 (2009).
32. Boylan, J. F. Radiopaque nitinol alloys for medical devices. *EUROPEAN PATENT.* 2039378A2
33. Venugopalan, R. & Trepanier, C. Assessing the corrosion behaviour of Nitinol for minimally-invasive device design. *Min Invas Ther & Allied Technol.* **9**, 67–74 (2000).
34. Steegmueller, R., Wagner, C., Fleckenstein, T. & Schuessler, A. Gold coating of nitinol devices for medical applications. *Mater Sci Forum* **161**, 394–395 (2002).

Acknowledgments

The authors thank Prof. B. M. Huang (BEIJING SMART TECHNOLOGY CO., LTD.) for great help in preparing the material. This work was supported by the key National Natural Science Foundation of China (NSFC) (51231008), the National 973 program of China (2012CB619403), the Science Foundation of China University of Petroleum, Beijing (No.2462013YJRC005), the Key Project of Chinese Ministry of Education (313055). The use of the Advanced Photon Source and the Center for Nanoscale Materials were supported by the US Department of Energy, Office of Science, and Office of Basic Energy Science under Contract No.DE-AC02-06CH11357.

Author contributions

L.S.C. and S.J.H. designed the research topic of this project. Y.R. and Y.D.W. supervised the synchrotron experiments. S.J.H., X.H.X., C.Y. and H.Z. carried out the synchrotron experiments. J.J. and F.M.G. carried out the material preparation and tensile experiments. S.J.H., Y.R., Z.H.C., D.Q.J., Y.Z.L. and D.E.B. wrote the manuscript.

Additional information

Supplementary information accompanies this paper at http://www.nature.com/scientificreports

Competing financial interests: The authors declare no competing financial interests.

How to cite this article: Hao, S. *et al.* A novel multifunctional NiTi/Ag hierarchical composite. *Sci. Rep.* **4**, 5267; DOI:10.1038/srep05267 (2014).